

Large zenith angle observations with the high-resolution GRANITE III camera

D. Petry¹ and the VERITAS Collaboration²

¹Dept. of Physics and Astronomy, Iowa State University, Ames, IA 50010, USA

²Whipple Observatory, Amado, AZ, 85645, USA

Abstract. The GRANITE III camera of the Whipple Cherenkov Telescope at the Fred Lawrence Whipple Observatory on Mount Hopkins, Arizona (2300 m a.s.l.) has the highest angular resolution of all cameras used on this telescope so far. The central region of the camera has 379 pixels with an individual angular diameter of 0.12° . This makes the instrument especially suitable for observations of gamma-induced air-showers at large zenith angles since the increase in average distance to the shower maximum leads to smaller shower images in the focal plane of the telescope. We examine the performance of the telescope for observations of gamma-induced air-showers at zenith angles up to 63° based on observations of Mkn 421 and using Monte Carlo Simulations. An improvement to the standard data analysis is suggested.

1 Introduction

By large-z zenith-angle observations we mean targeting an astronomical source with a ground-based telescope when it is more than 45° away from the zenith. Many authors have stressed the potential of using Imaging Atmospheric Cherenkov Telescopes (CTs) for observations of sources of high-energy γ -rays at large zenith angles (see e.g. Konopelko et al. (1999) and references therein). Several successful observations have already been made (e.g. Tanimori et al. (1998), Aharonian et al. (1999), Chadwick et al. (1999), Krennrich et al. (1999), Mohanty et al. (1999)).

Since the effective depth of the atmosphere increases to a good approximation as $1/\cos(\vartheta)$ (where ϑ denotes the zenith angle), the distance of the telescope to the shower maximum increases proportionally¹. The Cherenkov light produced in the shower illuminates a larger area on the ground which leads to an increase in the effective collection area of the CT. This increase should very roughly be as large as $1/\cos^2(\vartheta)$ but is in reality even larger due to changes in the shape of the

Correspondence to: petry@iastate.edu

¹Note that this approximation begins to break down at $\vartheta = 70^\circ$ due to the curvature of the earth.

lateral distribution of the Cherenkov photons density. The expected drawbacks of large- ϑ observations are an increased energy threshold and possibly worse background suppression since the average Cherenkov photon density caused by the shower at the telescope decreases with increasing ϑ roughly as $\cos^2(\vartheta)$. Furthermore, the angular extension of the shower image decreases. This means that with a given CT photomultiplier camera, the image is fainter and contained in fewer pixels. There is less information for distinguishing γ -induced showers from the hadronic background showers.

It is a priori not obvious by how much the gain in collection area will compensate for the decreasing image quality. A camera with higher angular resolution should suffer less from the effects of shrinking images. It is therefore especially interesting to investigate the performance of the new GRANITE III camera on the Whipple telescope (Mt. Hopkins, Arizona) which has an angular resolution of 0.12° in its central region, the best resolution ever available on this CT. This camera is described in Finley et al. (these proceedings).

In this article we derive the performance of GRANITE III as a function of the zenith angle ϑ and investigate possible improvements to the present standard data analysis which is optimized for small ϑ . We do this by examining the performance of the standard analysis at different zenith angles using simulated γ -showers and real telescope data from off-source observations. The improvements are then verified using observations of Mkn 421. It is especially helpful that Mkn 421 was in a high state during the observations.

2 Monte Carlo Data

The Monte Carlo (MC) data used in this study was specially produced using the simulation code described by Mohanty et al. (1998). The agreement of this MC data with the data obtained from the Whipple telescope in the 2000/2001 observing season was thoroughly tested. Special measurements of the telescopes point spread function, photomultiplier efficiency, light-cone collection efficiency and the photoelectron-to-digital-count conversion were made and the results inclu-

Table 1. Production parameters of the Monte Carlo data for γ -induced showers used in this study. E denotes the primary energy, r the impact parameter.

ϑ ($^\circ$)	20	40	48	54	58	62
$1/\cos(\vartheta)$	1.064	1.3	1.5	1.7	1.9	2.1
shower number	$8 \cdot 10^5$	$2 \cdot 10^5$	10^5	10^5	10^5	10^5
spectral index	2.5	2.5	2.5	2.5	2.5	2.5
min. E (GeV)	50	100	180	200	200	200
max. E (TeV)	100	100	100	100	100	100
max. r (m)	310	400	550	650	760	870

ded in the simulation (Krennrich et al. 2001). Realistic noise was added to the pixel values in order to simulate the night sky background light.

Since all shower image parameters are expected to change linearly with the average distance to the shower maximum which is in turn expected to scale with $1/\cos(\vartheta)$, the MC data was produced at equidistant values of $1/\cos(\vartheta)$. Table 1 gives an overview of the production parameters. Only gamma primaries were produced. For studies of hadronic showers, off-source observations with the Whipple telescope were used.

3 Data from the observation of Mkn 421 and off-source positions

The data was selected on the basis of the observer logs using the VERITAS online log sheet database. Only prime-weather data from 2000 or 2001 with no negative comments in the log sheets was accepted. A total of 7.0 h of Mkn 421 data with $6^\circ < \vartheta < 22^\circ$ (749801 events), 14.4 h of Mkn 421 data with $34^\circ < \vartheta < 64^\circ$ (1158149 events) and 14.5 h of off-source data with $6^\circ < \vartheta < 64^\circ$ (1074715 events) were used.

4 Data analysis and results

4.1 Telescope performance

The data was subjected to the standard Whipple telescope image processing which leads to a set of 7 parameters for each shower (ALPHA, LENGTH, WIDTH, DIST, SIZE, MAX1, MAX2). The cut on the signal in the two brightest pixels of the image (MAX1>15 and MAX2>12 photoelectrons) essentially determines the trigger threshold for γ -showers in the raw data. By applying the MAX1 and MAX2 cuts to the MC γ -shower dataset, the effective collection area for primary γ -rays after trigger of the Whipple telescope was calculated (Fig. 1).

The suppression of the hadronic background is achieved by applying cuts to all image parameters mentioned above. By optimizing on data obtained from Crab Nebula observations at $\vartheta < 30^\circ$, a set of standard cuts was obtained (see Finley et al., these proceedings). These so-called Supercuts 2001 are constant cuts which are neither functions of ϑ nor any other parameter. By applying these cuts to the MC γ -shower dataset, the effective collection area of the Whipple

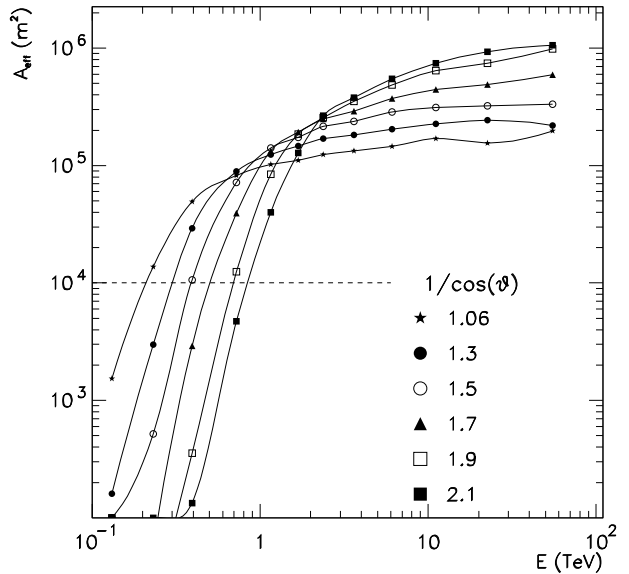


Fig. 1. The effective γ -ray collection area after trigger of the Whipple Telescope with the GRANITE III camera and the setup of the 2000/2001 observing period. Each curve shows the collection area of a different zenith angle (ϑ) as indicated by the symbols.

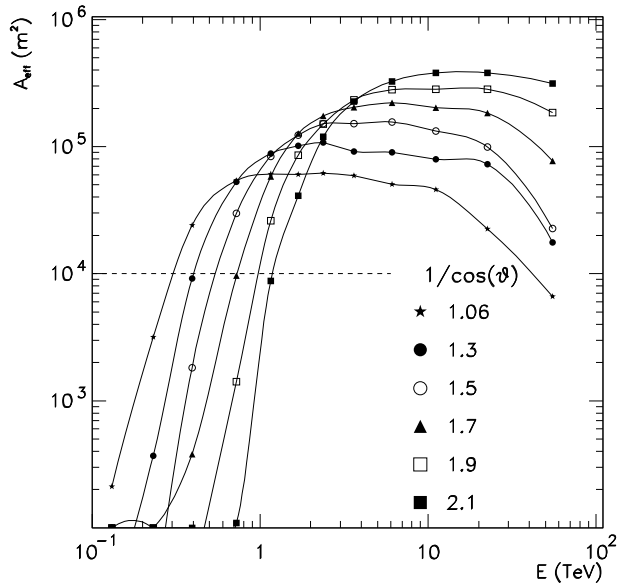


Fig. 2. As Fig. 1 but with the additional application of the Supercuts 2001 γ /hadron separation.

telescope was determined (Fig. 2).

By convoluting the collection areas in Fig. 2 with a power-law spectrum with index 2.7 and determining the energy at which the resulting rate peaks, one obtains the “energy of peak sensitivity” E_p for each zenith angle. The values are given in table 2.

Table 2. Values of the energy of peak sensitivity E_p for the Whipple Telescope in the 2000/2001 observing season using Supercuts2001.

$1/\cos(\vartheta)$	1.064	1.3	1.5	1.7	1.9	2.1
E_p (GeV)	380	520	790	1200	1500	2200

4.2 Possible improvements of the γ /hadron separation

Comparing Figs. 1 and 2, improvements seem possible mainly at large energies and not so much at large zenith angles. However, as Fig. 3 (left plot) shows, the background rejection of the Supercuts2001 deteriorates dramatically with increasing ϑ . We examine the individual image parameters in order to identify the reasons.

The ALPHA distribution after cuts has a shape which is independent of ϑ . The cut at 15° is optimal for all ϑ .

The DIST cut ($0.4^\circ < \text{DIST} < 1.0^\circ$) has (after all other cuts) a nearly ϑ -independent efficiency both for γ s and background (see Fig. 3). The peak of the DIST distribution for γ s before cuts moves towards smaller values as ϑ increases, but for the γ s below 0.4° the ALPHA distribution is so broad that more than 60% are eliminated by the ALPHA cut (for all ϑ). Also the energy resolution for events with small DIST is poor and since the solid angle is small, they constitute a small part of the total events. The upper DIST cut is determined by the field of view of the camera. It is therefore not necessary to vary the DIST cut with ϑ .

The lower cuts on WIDTH and LENGTH ($\text{WIDTH} > 0.05^\circ$ and $\text{LENGTH} > 0.09$) are dictated by the optics of the telescope and therefore nearly independent of ϑ . This is illustrated by Figs. 4 and 5. While their lower end remains at the same values, the WIDTH and LENGTH distributions become, however, more narrow as ϑ increases and a ϑ -independent cut has too large background efficiency (see also Fig. 3). The upper cuts on WIDTH and LENGTH ($\text{WIDTH} < 0.13^\circ$ and $\text{LENGTH} < 0.26$ in the Supercuts2001) are therefore the prime candidate for improving the background rejection.

Finally, the cut on LENGTH/SIZE ($< 1.3 \times 10^{-3} (\text{}/\text{photo-electron})$) shows a constant γ -efficiency and a decreasing background efficiency with increasing ϑ (see Fig. 3). Here,

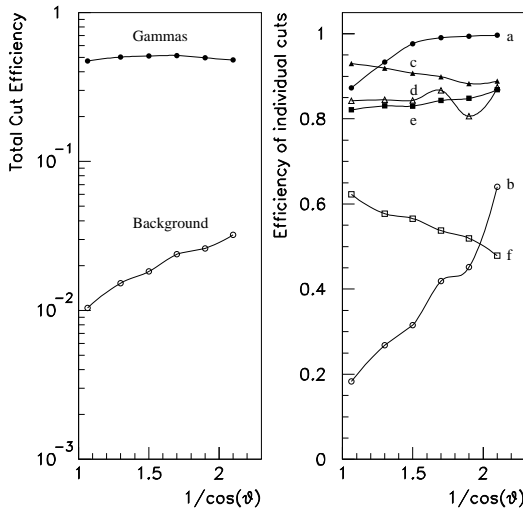


Fig. 3. The efficiency (eff.) of the Supercuts2001 for simulated γ s (solid symbols) and real background data (open symbols). Left: eff. of all cuts after the MAX1 & MAX2 cut. Right: (a, b) eff. of the upper LENGTH and WIDTH cuts after all other cuts, (c, d) eff. of the DIST cut after all other cuts, (e, f) eff. of the LENGTH/SIZE cut after all other cuts.

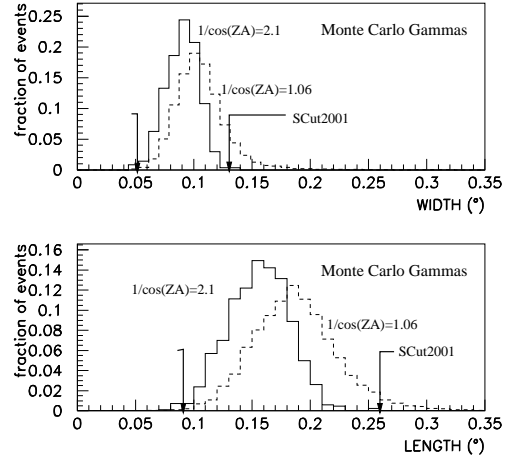


Fig. 4. Comparison of the WIDTH and LENGTH distributions (after all other cuts) of simulated γ events at small and large zenith angles. See text.

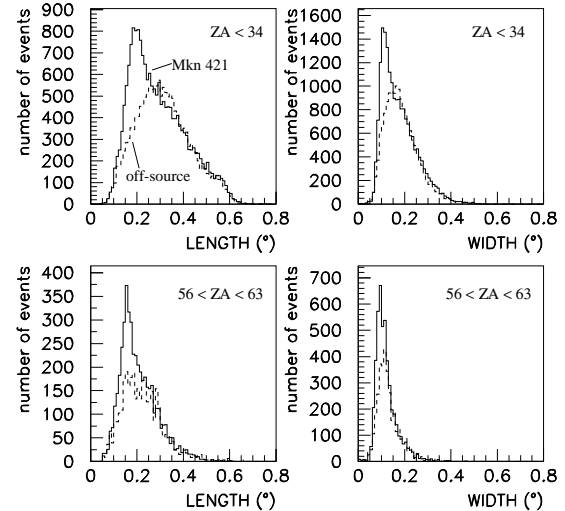


Fig. 5. Comparison of the WIDTH and LENGTH distributions (after all other cuts) for observations of Mkn 421 and off-source positions at small and large zenith angles. See text.

little improvement seems possible.

In order to improve the background rejection of the upper cuts on WIDTH and LENGTH, we examine as a function of ϑ the cut value with a γ -efficiency of 84%. Since both the WIDTH and the LENGTH distributions for pure γ s after cuts are Gaussian to a very good approximation, we determine the mean and the standard deviation of the simulated distributions at each value of ϑ by fitting a Gaussian. The sum of mean and standard deviation is then plotted versus $1/\cos(\vartheta)$ (Fig. 6).

As one would expect from the geometry of the shower observation, there is a linear dependence of the shower image size, and therefore also the WIDTH and LENGTH values under discussion, on $1/\cos(\vartheta)$. The result of a linear fit to the two groups of points is given in Fig. 6. In order to obtain

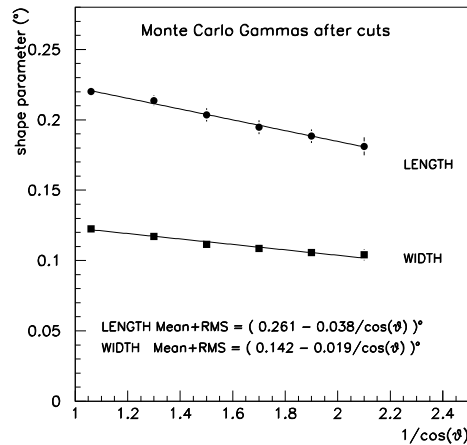


Fig. 6. The upper WIDTH and LENGTH cut values with γ -efficiency 84% as a function of $1/\cos(\vartheta)$. The cuts are calculated by adding one standard deviation to the mean of the distribution. See text.

an expression for ϑ -dependent upper cuts on WIDTH and LENGTH, we scale the two lines such that they assume the Supercuts2001 value at the zenith angle where the supercuts were optimized which is $\vartheta \approx 20^\circ$. The resulting cuts are:

$$\begin{aligned} \text{WIDTH} &< (0.15 - 0.020/\cos(\vartheta))^\circ \\ \text{LENGTH} &< (0.31 - 0.045/\cos(\vartheta))^\circ \end{aligned} \quad (1)$$

We replace the corresponding ϑ -independent cuts in the Supercuts2001 by the cuts in equation 1 and compare the performance of this new set of cuts (the “zenith-angle-dependent Supercuts”) with that of the standard Supercuts2001.

Fig. 7 shows that the ϑ -dependent cuts improve the background rejection by up to a factor 2 at the largest zenith angles while they reduce the γ -efficiency by only up to 10%. Furthermore, the overall quality factor (γ -efficiency divided

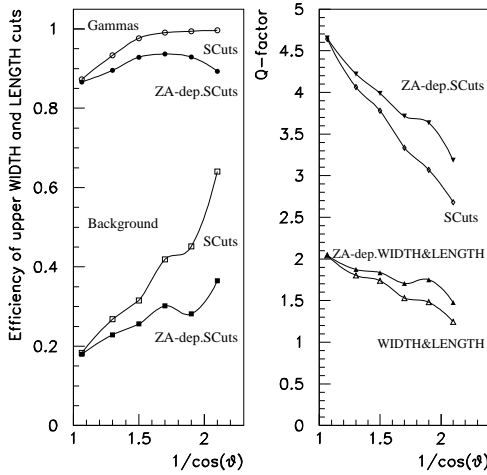


Fig. 7. (a) (left) The efficiency of the upper cuts on WIDTH and LENGTH after all other cuts for simulated γ s and real background data in the case the Supercuts2001 and the zenith-angle-dependent Supercuts derived here. (b) (right) The total quality factor of the whole set of cuts (upper two curves) and the quality factor of only the upper cuts on WIDTH and LENGTH after all other cuts.

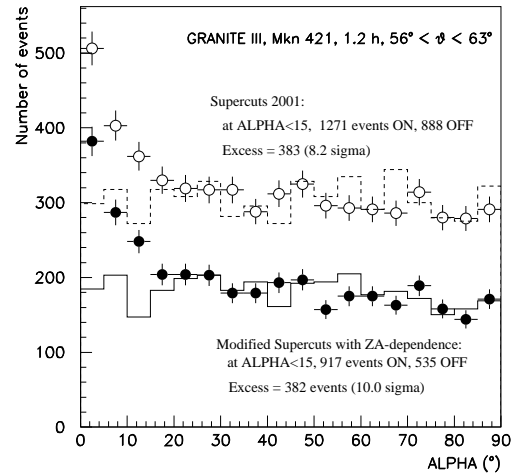


Fig. 8. The distribution of the orientation angle ALPHA for observations of Mkn 421 (symbols) and off-source observations (lines) after application of Supercuts2001 (upper curves) and the zenith-angle-dependent Supercuts derived here.

by the square-root of the background efficiency) drops from 4.7 to 2.7 for the standard Supercuts2001 when going from $\vartheta = 20^\circ$ to 60° , while it drops only to 3.2 when the ϑ -dependent cuts are used.

The improvement in sensitivity is verified using the Mkn 421 observations. Fig. 8 shows the result for the data at the largest ϑ available in this study. The expected improvement in significance from the Q-factors in Fig. 7 is $3.64/3.07 = 1.19$, the observed improvement is $10.0/8.2 = 1.21$. For intermediate zenith angles (45° - 56°) the expected improvement is $3.90/3.60 = 1.08$, in the Mkn 421 dataset we observe $15.1/14.2 = 1.06$. At smaller ϑ the two sets of cuts converge and no significant improvement is expected or observed.

5 Conclusion

We have quantified the performance of the GRANITE III camera on the Whipple Telescope and the current standard analysis at zenith angles $\vartheta < 63^\circ$ and identified improvements to the standard data analysis for $\vartheta > 45^\circ$.

Acknowledgements. The VERITAS Collaboration is supported by the U.S. Dept. of Energy, NSF, the Smithsonian Institution, PPARC (U.K.) and Enterprise-Ireland.

References

- Aharonian, F. et al., 1999, A&A 349, 29
- Chadwick, P.M., et al., 1999, J.Phys. G 25, 1749
- Konopelko, A., et al., 1999, J.Phys.G 25, 1989
- Krennrich, F., et al., 1999, ApJ 511, 149
- Krennrich, F., et al., 2001, VERITAS internal note.
- Mohanty, G., et al., 1998, Astropart. Phys 9, 15
- Mohanty, G., et al., 1999, in Kieda, D., Salamon, M. & Dingus, B. (eds.) “Proc. 26th ICRC”, OOG 2.2.03
- Tanimori, T., et al., 1998, ApJ 492, L33